



Open access Journal

International Journal of Emerging Trends in Science and TechnologyIC Value: 76.89 (Index Copernicus) Impact Factor: 4.219 DOI: <https://dx.doi.org/10.18535/ijetst/v4i8.14>

A Framework for Building Change Detection using Remote Sensing Imagery

Authors

Md. Abdul Alim Sheikh¹, Alok Kole², Tanmoy Maity³¹Dept. of Electronics & Comm. Engineering, Aliah University, Kolkata, India²RCC Institute of Information Technology, Kolkata, India³Dept. of Mining Machinery Engineering, Indian School of Mines, Dhanbad, India

Abstract

Change detection of building from high-resolution remote sensing images is an important and challenging research field in remote sensing. In this paper a novel technique for building change detection from remote sensing imagery is presented. First, The Morphological Building Index (MBI) features values are computed for each of the pair images from our datasets and then change of these two MBI images is measured to indicate the building change. For evaluation purpose, the experiments are carried on IKONOS and Quick Bird images. The results show that the proposed technique can attain acceptable correctness rates above 90% with overall errors fewer than 9%. Compared with state-of-the-art methods in building change detection; the proposed framework is computationally much more efficient while achieving better performance in terms of correctness, completeness, and quality.

Keywords— Accuracy Assessment, Building, Change Detection, High Resolution Satellite Image, Morphological Building Index (MBI), Remote Sensing.

1. Introduction

Remote sensing technology is an important tool to get useful information from earth surface features. Change detection [1] is a procedure to recognize variation in the images by analyzing the remote sensing data taken at different time over the same region. It has many applications such as building damage assessment, land -use and land-cover change [4], urban landscape design, assessment of regional environments, disaster management and Geospatial Information Systems updating [2, 3, 4]. With the advance of technology, and the improvement in remote sensing, the high resolution remote sensing imagery has been widely used in change detection [6]. This vast amount of remote sensing images needs automation to carry out the change detection jobs timely and cost effectively. In this regard, automatic building change detection from remote sensing imagery is an important work in that area as the manual processing is costly and time consuming.

Various techniques have been reported in the literature for the building change detection using remote sensing imagery. These techniques are basically divided into two core groups: multi temporal and mono-temporal methods [7]. Multi-temporal methods identify changes between the early and late images taken at two different times of the same region and in mono-temporal method; later data is only used for investigation. Image rationing, image differencing [5], principal component analysis and post-classification comparison are the frequently used methods in change detection studies [4, 8, 9, 10]. There are also several other techniques such as digital image classification, artificial neural networks, spectral mixture and texture and analysis to identify the change of buildings [4, 8, 9, 11, 12]. Although many hard works have been made to the development of building change detection techniques, still it is an open research problem in remote sensing. Now-a-days, much attention has been given on the extraction of features that can be used to extract buildings from remote sensing

images without the need of training data or complex segmentation processes.

This paper presents a building change detection technique from satellite images taken at two different times over the same region. In this proposed approach first object-specific discriminative features are extracted using MBI [12, 13, 14] feature index to automatically detect the existence of building from remote sensing images. The MBI features values are computed for the both images under experiment and then change of MBI value is taken to measure change information. The key benefit of MBI is that it has no need of any training data. Before doing this step, the pair of two images taken at two different times is pre-processed to geometrically adjust images, radiometric correction and co-register the min common coordinate system. The location of building change is displayed using a change detection map.

The rest of the paper is prepared as follows. Section 2 describes the design flow of the proposed approach with some theoretical overview of MBI and pseudocode of the proposed algorithm. The dataset used in this experiment is introduced in Section 3. Experimental results are reported in Section 4. Section 5 gives a comparison analysis. Section 6 concludes this paper with future direction.

2. Methodology

The design flow of the proposed method is shown in Fig. 1. Each step is described in this section.

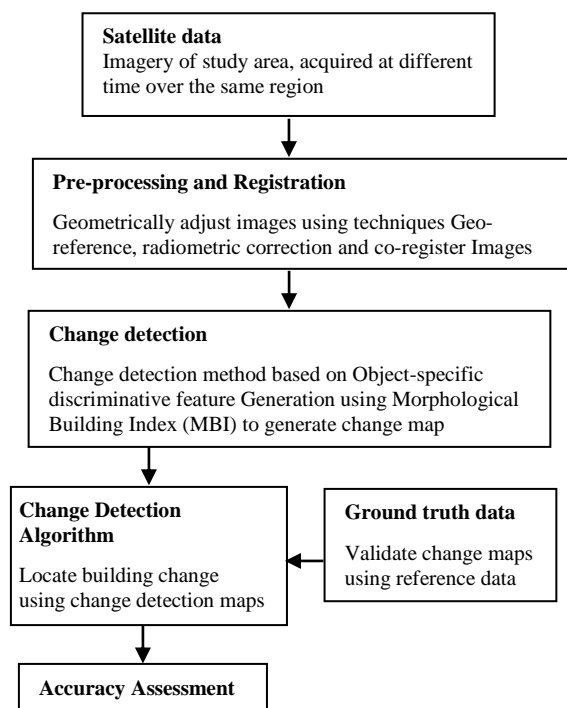


Fig. 1 Building Change Detection Methodology

2.1.Pre-processing

The pair of two images taken at two different times over the same region is pre-processed to eliminate geometric errors, and register them to a same coordinate system so that corresponding pixels represent the same objects. The process of image registration is done by ERDAS Imagine 2014. At the end, histogram matching technique is applied for the radiometric adjustment.

2.2.Change Detection

Building change information is measured using Morphological Building Indexed (MBI). A brief overview of MBI is presented. The location of building change detection is displayed using a change detection map. This step is illustrated in following sections 2.2.1 and 2.2.2.

2.2.1. Morphological Building Index (MBI) and Building detection

The MBI is used to extract the structural and spectral features of buildings with the help of morphological operators [12]. Change detection using MBI is carried out later. The calculation of MBI is summarized below:

Step 1) Calculation of brightness: It is computed by taking the highest value of all the spectral bands for each pixel b

$$= \max_{1 \leq k \leq K} (band_k(i, j)) \quad (1)$$

where $band_k(i, j)$ indicates the pixel (i, j) value of at the k -th band, and K is the number of visible bands.

Step 2) The structural and spectral features of buildings are represented by the differential morphological profiles (DMPs) of the top-hat filter (TH) with a sequence of Structural Elements (SE) [17].

The morphological white top-hat filter (TH) of the image f is given by f minus its opening.

$$W_TH_f(\theta, l) = f - R_f(f \ominus B(\theta, l)) \quad (2)$$

where $R_f(f \ominus B(\theta, l))$ represents the opening-by-reconstruction [18] of the image f . l and θ are the length and orientation of the structuring element B respectively.

Step 3) The morphological profiles (MPs) of the white top-hat are now defined as:

$$\begin{cases} MP_{W_TH}(\theta, l) = W_TH_f(\theta, l) \\ MP_{W_TH}(\theta, 0) = b \end{cases} \quad (3)$$

Step 4) Calculation of DMPs: the DMPs of top-hat filter

is given by

$$DMP_{W_TH}(\theta, l) = |W_TH_f(\theta, l) - W_TH_f(\theta, l - n)| \quad (4)$$

Where n is the interval of the profiles with $l (l_{min} \leq l \leq l_{max})$.

Step 5) The MBI is defined as the average of the DMPs of the white top-hat transformation [12]:

$$MBI = \frac{\sum_{\theta} \sum_l DMP_{W_TH}(\theta, l)}{D \times S} \quad (5)$$

where D and S are the total orientation and scale, respectively. Here, the number of orientations is set to $D=4$ (i.e. 45° , 90° , 135° , and 180°), and the scale is considered 11 (i.e., $2 \leq l \leq 52$ with $n = 5$)

Step 6) Detection of Building

Large MBI values in the DMP histogram of the top-hat filter indicate the structure to be buildings based on the fact that buildings have huge local contrast in different orientations and length, and the other structures are eliminated.

The building structures are extracted by the following rule, i.e.

$$I_b(i, j) = \begin{cases} 1, & MBI(i, j) > T_B \\ 0, & otherwise \end{cases} \quad (6)$$

Where $MBI(i, j)$ denotes building pixel value and T_B is the threshold MBI value for building.

Fig. 2 (a) Satellite Imagery (b) The Top–Hat DMP histogram of (a). The horizontal axis is the length and orientation of SE and the vertical axis is the DMP values of the Top –Hat filter

Fig. 2 shows the DMP histogram of the top-hat filter of a sample satellite imagery taking four classes as an example. It is a plot against DMP values vs. length for a particular direction. It is observed that in most of the magnitudes, the DMPs of the top-hat filter for buildings are notably larger

than the others. This is how the MBI can be used to identify buildings from images. After measuring the MBI values of the two images, the change of buildings from remote sensing imagery can be identified.

2.2.2. MBI Images for Change Detection

After measuring the MBI values of the two images taken at two different times, the change of buildings from remote sensing imagery can be identified. Suppose the MBI for the image taken at time T_1 is $MBI^{T1}(X_1)$ and the MBI for the image taken at T_2 is $MBI^{T2}(X_2)$. The variation of these two MBI images is measured to indicate the buildings change.

$$MBI(i, j) = |(MBI^{T1}(i, j) - MBI^{T2}(i, j))| \quad (7)$$

Where $MBI(i, j)$ gives the change of MBI value of pixel (i, j) at time T_1 and T_2 .

The building change detection rule is as follows:

$$Change(i, j) = \begin{cases} 1, & MBI(i, j) > TH_{MBI} \\ 0, & otherwise \end{cases} \quad (8)$$

Where $Change(i, j)$ represents whether the building pixels (i, j) is changed or not. The value 0 indicates for non-change and 1 for change, respectively. $MBI(i, j)$ is the change of MBI value of the two images under test. TH_{MBI} is the threshold of change.

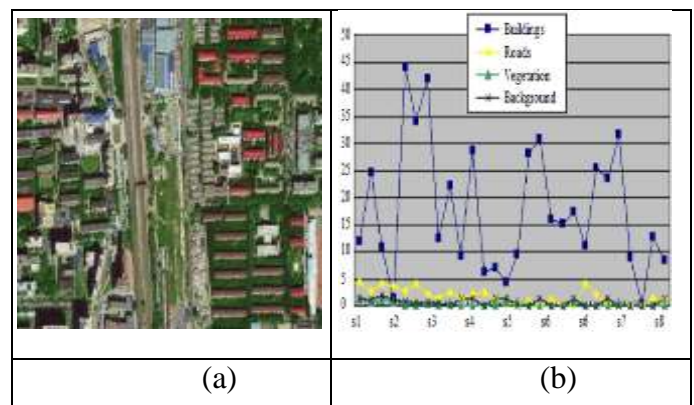


Table 1
Pseudocode of the Proposed Algorithm

Input:	Image X_1 and Image X_2 acquired at different time over the same region. Radiometric correction and co-register of the Images.
Output:	Building Change Detection Result
1.	MBI Calculation
1.1.	Calculate Brightest Image according to (1)
1.2.	For l ($l_{\min} \leq l \leq l_{\max}$)
1.3.	For $\theta = 1:1:D$
1.4.	$SE = \text{CreateStructureElement}(\theta, l)$
1.5.	$P = W_TH(SE, l, \text{image})$
1.6.	$Q = W_TH(SE, l-n, \text{image})$
1.7.	$DMP(\theta) = P - Q $
1.8.	End
1.9.	End
1.10.	$MBI = \frac{\sum_{\theta} \sum_l DMP_{WTH}(\theta, l)}{D \times S}$
1.11.	IF $MBI(i, j) > T_B$ THEN $I_b(i, j) = 1$ ELSE $I_b(i, j) = 0$ Where $MBI(i, j)$ denotes building pixel value and T_B is the threshold MBI value for building.
2.	Change Detection Based on MBI Value
2.1.	Calculate $MBI^{T1}(X_1)$ and $MBI^{T2}(X_2)$
2.2.	$MBI(i, j) = (MBI^{T1}(i, j) - MBI^{T2}(i, j)) $
2.3.	Set threshold value TH_{MBI}
2.4.	IF $MBI(i, j) \geq TH_{MBI}$ THEN $map(X_2, X_1) = 1;$ ELSE $map(X_2, X_1) = 0$ Where $MBI(i, j)$ indicate the change value of MBI of image X_1 and X_2 and $map(X_2, X_1)$ is building change map. $map(X_2, X_1)$ represents whether the object i is changed, with 0 and 1 for non-change and change, respectively.

3. Dataset

For evaluation the performance of the proposed approach, experiments were conducted on different sets of remote sensing images. For space limitation, only the results on three data sets are shown in this paper. The first dataset is pair of two IKONOS images taken over urban areas of central china in 2002 and 2009 [17]. The second data set is a pair of QuickBird images acquired in 2002 and 2005 taken over urban areas of central china [17].

The third dataset is a pair of QuickBird images [19] as shown in Fig. 3 (last row) taken over Beijing, acquired in September 2002 and November 2003.

4. Experimental Results

For evaluation the performance of the proposed technique, three satellite images are tested. A PC of CPU Intel (R) Core(TM) i5-4590 at 3.30 GHz and 4GB RAM is used to perform the experiments. The

method is realized in the MATLAB program. Three indices are used to quantify the performance values: correctness, completeness, and quality used by Peng. *et al.* [16].

$$\text{Correctness} = \frac{TP}{TP+FP} \quad (9)$$

$$\text{Completeness} = \frac{TP}{TP+FN} \quad (10)$$

$$\text{Quality} = \frac{TP}{TP+FP+FN} \quad (11)$$

Here, True Positive (TP) correspond to the change pixels that have been identified correctly; the False Positive (FP) indicates the pixels detected as changed but are actually not changed and False Negative (FN) represents the pixels identified as unchanged, but that however have changed.

The *correctness* value indicates the correct changed pixels. The *completeness* value indicates the ground truth changed pixels detected. Finally, the *quality* value indicates the goodness of the result. In calculating these values, manually formed reference data have been used. In Table 2, quantitative results are shown of the proposed method for the datasets.

Table 2
Quantitative Change Detection Results for the Data Sets by the Proposed Method

Datasets	Correctness	Completeness	Quality
IKONOS	93.23%	80.19%	76.68%
QuickBird1	83.97%	74.85%	70.23%
QuickBird2	91.38%	76.29%	72.15%

The changed maps of the three datasets are presented in Fig. 3. The results achieved by the proposed method can be taken as satisfactory compared with the ground truth map. Most of the changes are detected correctly in spite of some miss classification errors. The main advantage is that the whole design flow is carried out without ant training data. Both quantitative indices and visual results show that the proposed techniques attain acceptable results.

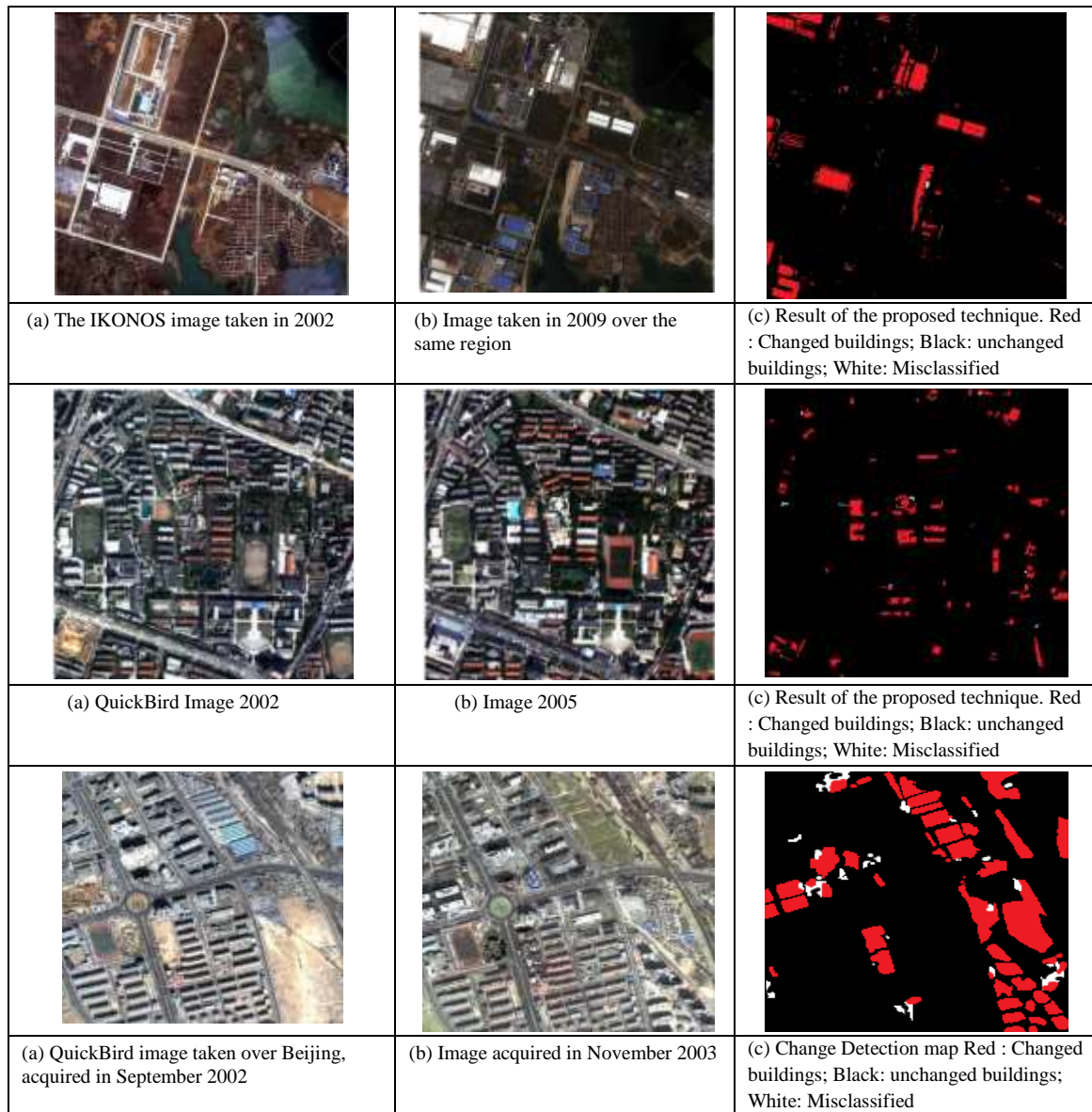


Fig. 3 The Change Detection Results of the proposed Technique. (a) Images Taken at Early Time and (b) Images Taken Later Time (c) The Changed Maps

5. Comparison Study

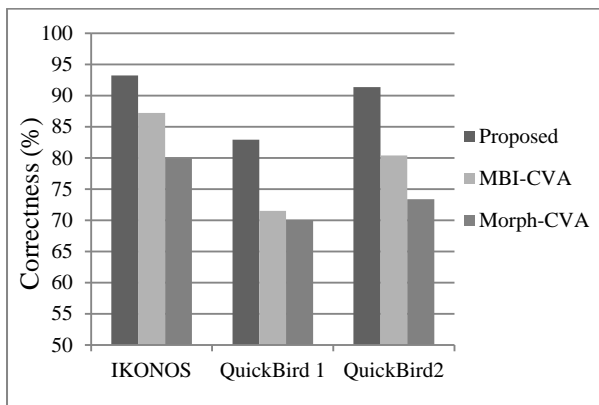
The proposed method is compared with two well-known change detection methods in Table 3. A comparison of the proposed method and with developed change detection methods revealed that the proposed method increased accuracy significantly.

The accuracy assessments of the four datasets are shown in Fig. 4(a)-(c), respectively, for the IKONOS, QuickBird1 and QuickBird2 images. The results show that, compared with other methods, the proposed method attains the highest correctness, completeness and quality in all the four tests

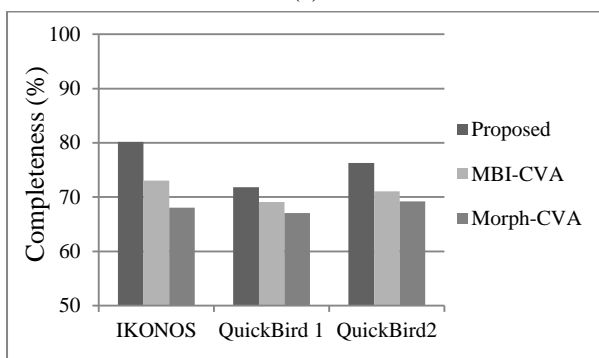
Table 3

Accuracy Comparison (%) for Building Change Detection Algorithms with our Proposed Method and the Other Two Methods MBI-based CVA (MBI-CVA) and Morphological CVA (Morph-CVA)

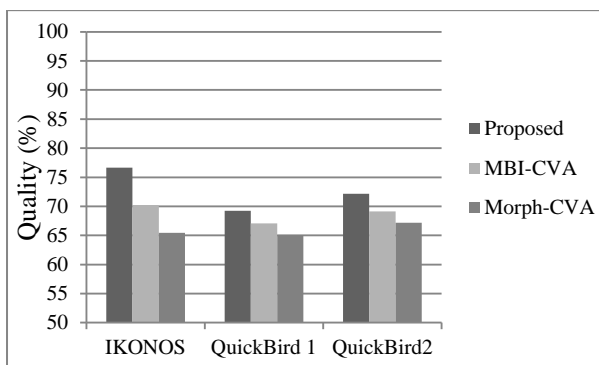
Methods	Correctness			Completeness			Quality		
	Data1 IKONOS	Data2 Quick Bird1	Data3 Quick Bird2	Data1 IKONOS	Data2 QuickBird1	Data3 QuickBird1	Data1 IKONOS	Data2 Quick Bird1	Data3 QuickBird2
Proposed	93.23	82.97	91.38	80.19	71.85	76.29	76.68	69.23	72.15
MBI-CVA	87.23	71.51	80.40	73.02	69.09	71.05	70.23	67.06	69.15
Morph-CVA	79.98	70.07	73.39	68.03	67.05	69.20	65.45	65.06	67.18



(a)



(b)



(c)

Fig. 4 Quantitative Evaluation and comparison of the proposed algorithm, MBI-CVA and Mor-CVA for change detection of buildings. (a) Correctness (b) Completeness and (c) Quality

VI. Conclusion

This paper proposes a novel change detection technique for building from remote sensing images. The method is to indicate the building change information based on the difference of MBI. The main novelties lie in the following aspects: 1) it needs no training data or complex segmentation processes that make the proposed approach very fast; 2) Object-specific change feature index make the proposed approach high in accuracy. The proposed method is validated on three pairs of remote sensing images: the IKONOS image and the

QuickBird data of urban areas. The experiments show that the proposed method can attain acceptable correctness rates above 90% with low total errors fewer than 9%. The visual and quantitative results validated the usefulness of the proposed framework.

References

1. Singh, A., Digital change detection techniques using remotely sensed data, *International Journal of Remote Sensing*, 10: 989–1003, 1989.
2. Radoi, Anamaria and Datcu, Mihai., Automatic Change Analysis in Satellite Images Using Binary Descriptors and Lloyd–Max Quantization, *IEEE Geoscience and Remote Sensing Letters*, 12(6): 1223–1227, 2015.
3. Tian, J., Cui, S. and Reinartz P., Building change detection based on satellite stereo imagery and digital surface models, *IEEE Trans. Geosci. Remote Sens.*, 51(1): 406–417, 2013
4. Lu, P. Mausel, E. Brond'izio, and E. Moran, Change Detection techniques, *Int. J. Remote Sens.*, 25(12): 2365–2401, 2004.
5. L. Bruzzone and D. F. Prieto, Automatic analysis of the difference image for unsupervised change detection, *IEEE Trans. Geosci. Remote Sens.*, 38(3):1171–1182, 2000.
6. Coppin, P., Jonckheere, I., K. Nackaerts, B. Muys, and E. Lambin, Digital change detection methods in ecosystem monitoring: A review, *Int. J. Remote Sens.*, 25(9): 565–1596, 2004.
7. Dong, L., Shan, J., A Comprehensive Review of Earthquake-induced Building Damage Detection with Remote Sensing Techniques, *.ISPRS Journal of Photogrammetry and Remote Sensing*, 85–99, 2013.
8. F. Pacifici and Frate, F. Del., Automatic change detection in very high resolution images with pulse-coupled neural networks, *IEEE Geosci. Remote Sens. Lett.*, 7(1): 58–62, 2010.
9. R. J. Radke, S. Andra, O. Al-Kofahi, and B. Roysam., Image change detection algorithms:

- Systematic survey, *IEEE Trans. Image Process.*, 14(3): 294–307, 2005.
10. Wang, Tian-Lin. and Jin ,Ya-Qiu., Postearthquake Building Damage Assessment Using Multi-Mutual Information From Pre-Event Optical Image and Post event SAR Image, *IEEE Geoscience and Remote Sensing Letters*, 9(3): 452-456, 2012.
 11. L. Gueguen, P. Soille. and Pesaresi, M., Change detection based on information measure, *IEEE Trans. Geosci. Remote Sens.*, 49(11): 4503–4515, 2011.
 12. Xing Huang, L. Zhang and Zhu, T., Building Change detection from multitemporal High-Resolution Remotely Sensed images based on a Morphological Building Index, *IEEE J.Sel.Topics Appl. Earth Observ. Remote Sens.*, 7(1): 105–115, 2014.
 13. X. Huang and L. Zhang, A multidirectional and multiscale morphological index for automatic building extraction from multispectral GeoEye-1 imagery, *Photogramm. Eng. Remote Sens.*, 77(7):721–732, 2011.
 14. X. Huang and L. Zhang., Morphological building/shadow index for building extraction from high-resolution imagery over urban areas', *IEEE J. Sel. Topics Appl. Earth Obs. Remote Sens.*, 5(1): 161–172, 2012.
 15. M. Pesaresi and J. A. Benediktsson., A new approach for the morphological segmentation of high-resolution satellite imagery, *IEEE Trans Geosci. Remote Sens.*, 39(2):309–320, 2001
 16. Peng,, T., Jermyn, I. H., V. Prinnet, and Zerubia, J., Incorporating Generic and Specific Prior Knowledge in a MultiscalePhase Field Model for Road Extraction from VHR Images, *IEEE J. Sel. Topics Appl. Earth Observ. Remote Sens.*, 1(2): 139–146, 2008.
 17. Yuqi Tang, Xin Huang, and Liangpei Zhang., Fault-Tolerant Building Change Detection From Urban High-Resolution Remote Sensing Imagery, *IEEE Geoscience and Remote Sensing Letters*, 10(5): 160-1064, 2013.
 18. R. C. Gonzalez, R. E Woods, *Digital image processing, Second Edition*, ISBN 0-201-18075-8, 2002.
 19. Huo, C., Zhou, Z., and Lu, H., Fast object-level change detection for VHR Images, *IEEE Geosci. Remote Sens. Lett.*, 7: 118–122, 2010.